population change across multiple populations, and asks how large the 'average' change in population size is over time; the latter method simply measures trends in individual populations, and asks whether the ratio of declining populations to increasing populations is significantly different from 1:1. The first method is preferable, because it allows us to assess potential changes in the rate of decline over time, but it requires large sample sizes that were not available for some regions. The second method allowed us to test for declines in those regions with small sample sizes.

ΔN method

This method was used to test for trends in the 'global' set, and to test for 'regional' trends in North America and western Europe (including the UK). For 'global' and 'regional' trends we calculated $\log (N+1)_{t+1} - \log (N+1)_t = \Delta N$ for successive yearly intervals. For this analysis, only populations having at least two consecutive years of data could be used. We then calculated $\bar{\Delta}N \equiv (\Sigma_{i=1}^{n} \Delta N)/n$ based on all populations (n) for which there were data for the time interval (t, $t+1$) in question (because the number of studies increases over time, so does the sample size for $\bar{\Delta}N$). This procedure was repeated for each year from 1950 to 1997, and the annual averages used to compute the cumulative average change, $\Delta N \equiv \Sigma_{t_0}^{t} \bar{\Delta}N$, from $T = 1950$ to $T = 1997$. More than 200 western European population time series come from two large studies in Sweden and Switzerland. Analyses of population trends with and without these data indicate they had no qualitative effect on the results.

Visual examination of a plot of $\bar{\Delta}N$ for the global set suggests three qualitatively different time periods, corresponding roughly to 1950–1960, 1960–1970 and 1970–1997. To estimate switchpoints between periods, we fitted regression models including dummy (categorical) variables defining the period intervals (for example, period 1: 1950–1960; period 2: 1961–1970, and so on). Changing the beginning and end points for a given period results in a change in model fit, with the best estimate of the switchpoints derived from the model with the lowest residual mean square. The initial switchpoints were selected by examination of the data, with subsequent fitting based on moving the switchpoints forwards and backwards from the initial estimate(s). Model fitting ended when models with switchpoints two years earlier and later than the best model had higher residual mean-square values. Our best-fit model partitioned the global set into three time periods: 1950–1960, 1960–1966 and 1966–1997. The best model for the western European data showed two distinct time periods (1960–1966 and 1966–1997), while the best model for North America showed a single trend from 1960 to 1997.

$\bar{\Delta}N$s are summary data. As such, using it as the dependent variable in regression underestimates the true error sums of squares. We have corrected for this by including the error contribution of each ΔN to $\bar{\Delta}N$ (ref. 29), and all significance tests use this true error sum of squares and the corresponding true degrees of freedom.

Proportion of declining populations method

In a second analysis, we evaluated trends in population size over time using the Spearman correlation, the Pearson correlation coefficient and Kendall's τ. Irrespective of the test statistic used, results were qualitatively the same. We present our results using Kendall's τ because it avoids some of the assumptions about data distribution. We calculated the correlation (Kendall's τ) between population size and year for each population in a particular geographical region. Populations were then classified as to whether they were declining (negative correlation), increasing (positive correlation) or had no trend (correlation = 0). For a population to show no trend, the correlation must be exactly 0. A log-linear model was fitted using the independent variables region, trend and their interaction (region × trend). Populations showing no trend were not included in the log-linear model. For the 'global' dataset and the three subsets, the Eastern European and African/Middle Eastern regions are presented but not included in the log-linear model; for the ≥7 year data set, Asia, South America and Australia/New Zealand are also presented, but excluded from the log-linear model because of low sample sizes.

Received 19 October 1999; accepted 26 January 2000.

1. Wake, D. B. Declining amphibian populations. *Science* **253,** 860 (1991).
2. Blaustein, A. R. & Wake, D. B. Declining amphibian populations: A global phenomenon? *Trends Ecol. Evol.* **5,** 203–204 (1990).
3. Blaustein, A. R., Wake, D. B. & Sousa, W. P. Amphibian declines: judging stability, persistence, and susceptibility of populations to local and global extinctions. *Conserv. Biol.* **8,** 60–71 (1994).
4. Wake, D. B. & Morowitz, H. J. Declining amphibian populations—a global phenomenon? Findings and recommendations. *Alytes* **9,** 33–42 (1991).
5. Pechmann, J. H. K. & Wilbur, H. M. Putting declining amphibian populations in perspective: natural fluctuations and human impacts. *Herpetologica* **50,** 65–84 (1994).
6. Lips, K. R. Decline of a tropical montane amphibian fauna. *Conserv. Biol.* **12,** 106–117 (1998).
7. Harte, J. & Hoffman, E. Possible effects of acidic deposition on a Rocky Mountain population of the tiger salamander *Ambystoma tigrinum*. *Conserv. Biol.* **3,** 149–158 (1989).
8. Corn, P. S. & Fogleman, J. C. Extinction of montane populations of the northern leopard frog (*Rana pipiens*) in Colorado. *J. Herpetol.* **18,** 147–152 (1984).
9. Pechmann, J. H. K. *et al.* Declining amphibian populations: The problem of separating human impacts from natural fluctuations. *Science* **253,** 892–895 (1991).
10. Meyer, A. H., Schmidt, B. R. & Grossenbacher, K. Analysis of three amphibian populations with quarter-century long time-series. *Proc. R. Soc. Lond. B* **265,** 523–528 (1998).
11. Hecnar, S. J. & M'Closkey, R. T. Spatial scale and determination of species status of the green frog. *Conserv. Biol.* **11,** 670–682 (1997).
12. Hecnar, S. J. & M'Closkey, R. T. Regional dynamics and the status of amphibians. *Ecology* **77,** 2091–2097 (1996).
13. Weygoldt, P. Changes in the composition of mountain stream frog communities in the Atlantic mountains of Brazil—frogs as indicators of environmental deteriorations. *Stud. Neotrop. Fauna Environ.* **24,** 249–255 (1989)
14. Berger, L. *et al.* Chytridiomycosis causes amphibian mortality associated with population declines in the rain forests of Australia and Central America. *Proc. Natl Acad. Sci. USA* **95,** 9031–9036 (1998).
15. Pounds, J. A., Fogden, M. P. L., Savage, J. M. & Gorman, G. C. Tests of null models for amphibian declines on a tropical mountain. *Conserv. Biol.* **11,** 1307–1322 (1997).
16. Laurance, W. F., McDonald, K. R. & Speare, R. Epidemic disease and the catastrophic decline of Australian rain forest frogs. *Conserv. Biol.* **10,** 406–413 (1996)
17. Drost, C. A. & Fellers, G. M. Collapse of a regional frog fauna in the Yosemite area of the California Sierra Nevada, USA. *Conserv. Biol.* **10,** 414–425 (1996).
18. Pounds, J. A., Fogden, M. P. L. & Campbell, J. H. Biological response to climate change on a tropical mountain. *Nature* **398,** 611–615 (1999).
19. Beebee, T. J. C. *et al.* Decline of the natterjack toad *Bufo calamita* in Britain: paleoecological, documentary and experimental evidence for breeding site acidification. *Biol. Conserv.* **37,** 59–71 (1990).
20. Carey, C. Hypothesis concerning the causes of the disappearance of boreal toads from the mountains of Colorado. *Conserv. Biol.* **7,** 355–362. (1993).
21. Cunningham, A. A. *et al.* Unusual mortality associated with poxvirus-like particles in frogs (Rana temporaria). *Vet. Rec.* **133,** 141–142 (1993).
22. Blaustein, A. R. *et al.* Effects of ultraviolet radiation on amphibians: Field experiments. *Am. Zool.* **38,** 799–812 (1998).
23. Kiesecker, J. M. & Blaustein, A. R. Synergism between UV-B radiation and a pathogen magnifies amphibian embryo mortality in nature. *Proc. Natl Acad. Sci. USA* **92,** 11049–11052 (1995).
24. Long, L. E., Saylor, L. S. & Soule, M. E. A pH/UV-B synergism in amphibians. *Conserv. Biol.* **9,** 1301–1303 (1995).
25. Wake, D. B. Action on amphibians. *Trends Ecol. Evol.* **13,** 379–380 (1998).
26. Tyler, M. J. Declining amphibian populations: a global phenomenon? An Australian perspective. *Alytes* **9,** 43–50 (1990).
27. Green, D. M. in *Amphibians in Decline: Canadian Studies of a Global Problem* (ed. Green, D. M.) 291–308 (Society for the Study of Amphibians and Reptiles, Lawrence, USA, 1997).
28. Englund, G., Sarnelle, O. & Cooper, S. D. The importance of data-selection criteria: meta-analysis of stream predation experiments. *Ecology* **80,** 1132–1141 (1999).
29. Draper, N. R. & Smith, H. *Applied Regression Analysis* 2nd edn (Wiley and Sons, New York, 1981).
30. Heyer, W. R., Donnelly, M. A., McDiarmid, R. W., Hayak, L. A. C. & Foster, M. S. (eds) *Measuring and Monitoring Biological Diversity: Standard Methods for Amphibians* (Smithsonian Institute Press, Washington, 1994).

Supplementary Information is available on *Nature*'s World-Wide Web site (http://www.nature.com) or as paper copy from the London editorial office of *Nature*.

Acknowledgements

We thank all the researchers who contributed amphibian population data and, in particular, J. Loman, T. Beebee and S. Zumbach for large unpublished data sets. This work was supported by Wildlife Habitat Canada, the Natural Sciences and Engineering Research Council of Canada, and the Schweizerischer Nationalfonds.

Correspondence and requests for materials should be addressed to J.E.H (e-mail: jeffhoul@science.uottawa.ca).

The metapopulation capacity of a fragmented landscape

Ilkka Hanski & Otso Ovaskainen

Department of Ecology and Systematics, PO Box 17 (Arkadiankatu 7), FIN-00014 University of Helsinki, Finland

Ecologists and conservation biologists have used many measures of landscape structure[1–5] to predict the population dynamic consequences of habitat loss and fragmentation[6–8], but these measures are not well justified by population dynamic theory. Here we introduce a new measure for highly fragmented landscapes, termed the metapopulation capacity, which is rigorously derived from metapopulation theory and can easily be applied to real networks of habitat fragments with known areas and connectivities. Technically, metapopulation capacity is the leading eigenvalue of an appropriate 'landscape' matrix. A species is predicted to persist in a landscape if the metapopulation capacity of that landscape is greater than a threshold value determined by the properties of the species. Therefore, metapopulation capacity can conveniently be used to rank different landscapes in terms of their capacity to support viable metapopulations. We present an empirical example on multiple networks occupied by an

endangered species of butterfly. Using this theory, we may also calculate how the metapopulation capacity is changed by removing habitat fragments from or adding new ones into specific spatial locations, or by changing their areas. The metapopulation capacity should find many applications in metapopulation ecology, landscape ecology and conservation biology.

The most basic aspects of metapopulation persistence in fragmented landscapes have been analysed with simple spatially implicit models[9], akin to models of infectious disease in homogeneous populations[10]. In the Levins model[11], assuming that a fraction h of habitat patches is suitable for occupancy, the equilibrium fraction of occupied patches (out of suitable patches) is given by

$$p^* = 1 - \frac{\delta}{h} \quad (1)$$

where δ is the ratio of the extinction and colonization rate parameters: $\delta = e/c$ (refs 9 and 12–15). A well known limitation of this and other spatially implicit models is that they cannot be used to analyse explicit spatial patterns. For example, if we assume that colonization is distance-dependent, simulation studies have shown that it makes a big difference to metapopulation persistence whether habitat loss (decreasing value of h) occurs randomly or non-randomly in space[16,17].

A spatially realistic version of the Levins model for a finite number of habitat patches of known areas and spatial locations can be constructed by modelling the rate of change in the probability of patch i being occupied as[18]:

$$\frac{dp_i(t)}{dt} = (\text{Colonization rate}_i)[1 - p_i(t)] - (\text{Extinction rate}_i)p_i(t) \quad (2)$$

The theory developed here is general and not restricted to particular functional forms of the colonization and extinction rates, but for the purpose of illustration we use here specific assumptions that are simple and biologically well justified, namely Extinction rate$_i = e/A_i$ and Colonization rate$_i = c\Sigma_{j\neq i}\exp(-\alpha d_{ij})A_j p_j(t)$, where A_i is the area of patch i, d_{ij} is the distance between patches i and j, $1/\alpha$ is the average migration distance, and e and c are constants (for justification, see Methods). With these or other comparable assumptions, the most important metapopulation processes, colonization and extinction, can be related to the most important structural features of fragmented landscapes, patch areas and spatial locations[9,19].

We turn to matrix notation to describe the system of equations giving the rates of change for the p_i values. Using the above assumptions in equation (2), matrix $\mathbf{M}$ consists of elements $m_{ij} = \exp(-\alpha d_{ij})\ A_i A_j$ for $j \neq i$ and $m_{ii} = 0$. It can be shown that an equilibrium solution with $p_i^* > 0$ for all i exists if and only if

$$\lambda_{\mathbf{M}} > \delta \quad (3)$$

where $\lambda_{\mathbf{M}}$ is the leading eigenvalue of matrix $\mathbf{M}$. Equation (3) thus gives the condition for persistence of a species in a given landscape.

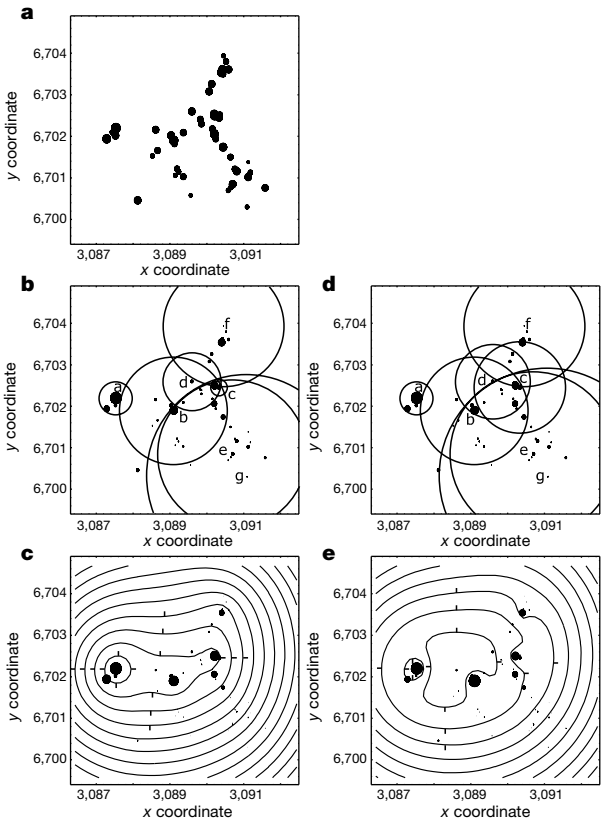

Figure 1 Change in metapopulation capacity due to removal of a patch or addition of a new patch in a particular spatial location within the existing patch network. Data based on equation (6). **a–c**, The sizes of the dots (habitat patches) are proportional to the logarithm of patch area (**a**), patch area (**b**) and the value of λ_i (**c**). The contour lines in **c** indicate the level of increase (decrease) in metapopulation capacity, corresponding to a 30% difference in patch areas, that would result from placing a new patch (removing an existing patch) in a particular location. For the explanation of the circles around patches a–g in **b** see Methods and Fig. 2. **d**, **e**, As in **b** and **c**, but here the model includes regional stochasticity, implemented as explained in Methods ($\gamma = 1$, $\beta = \alpha = 1$). The tick marks on the contour lines indicate the direction of the slope. *x* coordinate, longitude; *y* coordinate, latitude.

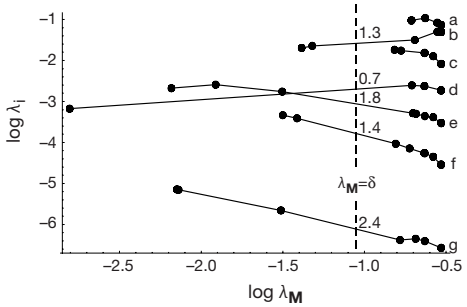

Figure 2 The contribution of patch i to $\lambda_{\mathbf{M}}$, $\lambda_i \equiv x_i^2\lambda_{\mathbf{M}}$, calculated for increasingly large regions around patches a–g in Fig. 1b (see Methods). The corresponding pairs of λ_i and $\lambda_{\mathbf{M}}$ are shown by dots from left to right, joined by a line for each patch. The broken vertical line gives the threshold condition estimated in Fig. 3, defining the size of the circle around the patch in Fig. 2b.

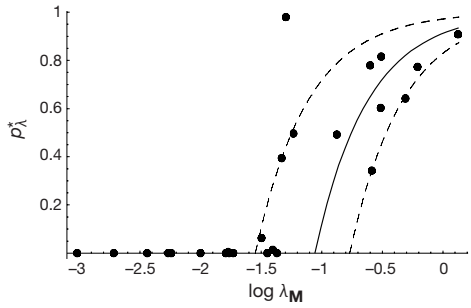

Figure 3 Plot of p_λ^* against the logarithm of metapopulation capacity ($\lambda_{\mathbf{M}}$) in 25 real patch networks that are potentially occupied by the Glanville fritillary butterfly (*Melitaea cinxia*) in the Åland Islands in southwest Finland[30]. The continuous line is based on the average of the estimated δ values for networks with $p_\lambda^* > 0.3$. The broken lines give the minimum and maximum estimates, but omitting the two networks yielding the most extreme values.

An analogous threshold condition is well established in epidemiological theory[10,20] for the spread of an infectious disease, although the epidemiological models are generally structured by factors such as sex or age rather than by the spatial location of populations. The threshold condition has been previously discussed in the context of metapopulation dynamics by Adler and Nüernberger[21].

An appropriately weighted average of the p_i^* values can be closely approximated by

$$p_\lambda^* = 1 - \frac{\delta}{\lambda_M} \quad (4)$$

We note the structural identity between equations (1) and (4). In the spatially realistic model, λ_M plays exactly the same role as h, the amount of suitable habitat, plays in the simple Levins model (equation 1), in which all patches are identical and equally connected, and in which the spatial arrangement of patches therefore makes no difference. We term λ_M the metapopulation capacity of a fragmented landscape: λ_M is a measure that captures the impact of landscape structure—the amount of habitat and its spatial configuration—on metapopulation persistence. λ_M has to exceed a threshold value that is set by the properties of the species (δ) for long-term persistence (equation 3). To compute λ_M for a particular landscape, only the spatial scale of connectivity (set by the species parameter α) and the areas and the spatial locations of the habitat fragments need to be known. For a given landscape, λ_M increases with decreasing α, because small α strengthens connectivity. When α is very small, patches will contribute to λ_M in relation to their areas only. For a given species (constant α), λ_M allows a straightforward comparison of multiple fragmented landscapes, which can be conveniently ranked in terms of their capacity to support a viable metapopulation. Such comparisons are essential for management-oriented and spatially extended population viability analyses[22,23].

The metapopulation capacity is, to a good approximation, a sum of contributions from individual habitat fragments. The contribution of fragment i is given by $\lambda_i \equiv x_i^2 \lambda_M$, where x_i is the ith element in the leading eigenvector of matrix $\mathbf{M}$ (see Methods). λ_i thus measures the significance of habitat fragment i to the threshold condition for metapopulation persistence. Conveniently, we can also assess how adding a new patch with area A_k to a specific location in the landscape would increase λ_M (Fig. 1; see Methods).

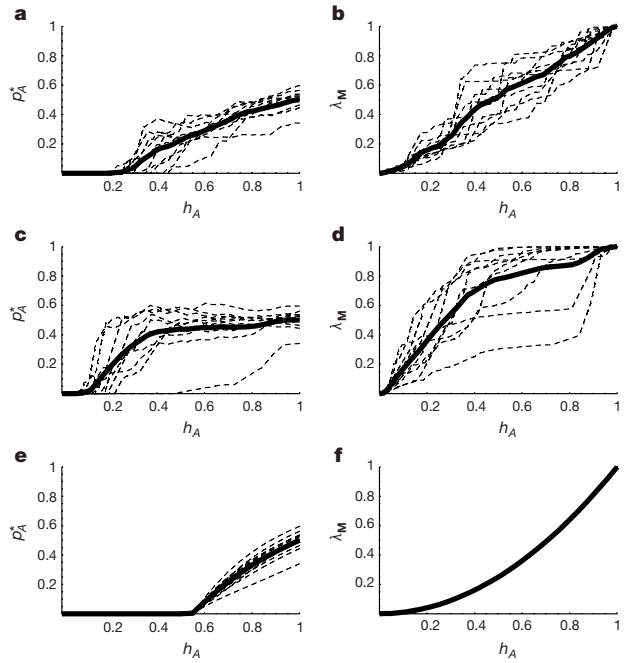

Figure 4 Consequences of habitat loss on patch occupancy and the threshold value for metapopulation persistence. Three scenarios are shown: **a**, **b**, random loss of habitat patches; **c**, **d**, systematic (non-random) loss of patches; **e**, **f**, loss of area from each existing patch. For each scenario the fraction of occupied habitat (p_A^*) is plotted against the fraction of suitable habitat (h_A) (**a**, **c**, **e**) and the relationship between λ_M and h_A (see Methods) is shown (**b**, **d**, **f**). Solid lines, average.

The above results should find useful applications in the development of algorithms for designing nature reserves[24,25], where the spatial dynamics of the focal species in the reserve network have typically not been considered. In the epidemiological context, λ_i gives the contribution of the given group of individuals to the spread of the disease, and could thus be used to rank, for example, vaccination scenarios. However, it is necessary to pay close attention to what λ_i really measures—the contribution of fragment i to λ_M at the threshold for deterministic persistence. In a large network with aggregated distribution of habitat patches, one particular cluster of patches will be the stronghold for the metapopulation in the entire network, and hence the properties of this cluster will largely set the threshold condition. The spatially more localized significance of individual patches can be examined by, for example, calculating the λ_M and λ_i values for smaller and larger regions around each patch (Fig. 2; see Methods). Patches that are located in the less significant patch clusters from the viewpoint of metapopulation persistence in the entire network may nonetheless have substantial significance in their own neighbourhood (for example, patches e and f in Figs 1 and 2). It is also possible to define and compute measures related to λ_M that characterize the impact of landscape structure on metapopulation invasion or on metapopulation size rather than on metapopulation persistence (O.O. & I. H., manuscript in preparation).

We now return to the nature of the weighted average of patch occupancy probabilities in equation (4). This equation is obtained when the p_i^* values are weighted by the relative contributions of the habitat fragments to metapopulation capacity, that is, $p_\lambda^* = \Sigma \lambda_i p_i^* / \lambda_M$. Thus p_λ^* gives the fraction of λ_M that is 'used' by the species at equilibrium. Following the general notion[26] that the threshold condition for persistence of a consumer is given by the amount of unused limiting resource at equilibrium, we can calculate the threshold value of λ_M for metapopulation persistence as $\delta = \lambda_M(1-p_\lambda^*)$, which gives a heuristic derivation of equation (4).

As an example, Fig. 3 shows p_λ^* against λ_M for 25 real patch networks potentially occupied by the Glanville fritillary butterfly (*Melitaea cinxia*) in the Åland Islands in southwest Finland. Using the formula $\delta = \lambda_M(1-p_\lambda^*)$, the threshold value was estimated for networks with $p_\lambda^* > 0.3$ (see Methods). The average value of these relatively independent estimates predicts well the absence or near absence of the species in the remaining networks (continuous line in Fig. 3).

Our model can also be used to examine the consequences of habitat loss on metapopulation persistence. Let p_A^* be the average patch occupancy probability weighted by patch area. p_λ^* gives a reasonably good approximation of p_A^*, though it tends to give an overestimate (O.O. & I. H., manuscript in preparation). The exact value of p_A^* can be calculated by first solving the values of p_i^* by iteration[27]. If h_A is the fraction of the pooled habitat area that remains suitable for occupancy, the fraction of unused habitat (out of the original amount of habitat) at equilibrium is given by

$$\text{Amount of empty habitat} = h_A(1 - p_A^*) \approx \frac{h_A \delta}{\lambda_M} \quad (5)$$

(assuming that $p_A^* \approx p_\lambda^*$). In the Levins model the amount of empty habitat remains constant for $h > \delta$ (see equation (1) and refs 9, 12 and 14). This is approximately so in the present model if habitat loss is random, in which case λ_M decreases roughly in proportion to the decrease in the amount of suitable habitat, h_A (Fig. 4b). In contrast, if habitat is lost in large blocks, λ_M decreases initially less than in proportion to the decrease in h_A, as metapopulation dynamics in the remaining habitat are affected relatively little (Fig. 4d). Therefore, such non-random loss of habitat is less detrimental to metapopulation

persistence than random loss of habitat (compare Figs. 4a and c; this conclusion must naturally be applied cautiously to real landscapes and populations, because they may be affected by processes not included in the model). The present model can be used to investigate the consequences of any pattern of habitat loss, for example, decreasing areas of the existing fragments, which is often even more harmful to metapopulation persistence (Fig. 4e) than random loss of entire patches (Fig. 4a).

The examples presented here illustrate how metapopulation capacity can be used to examine both the local and the global aspects of metapopulation persistence in real fragmented landscapes. We expect that metapopulation capacity will find many constructive applications in metapopulation ecology, landscape ecology and conservation biology. □

Methods

The model structure

We have used here a specific spatially realistic version of the Levins model to illustrate the concept of metapopulation capacity. The numerical results are model-specific, because λ_M integrates the effects of landscape structure on metapopulation processes as specified by a dynamic model, but the theory is general and results can be readily obtained for a range of continuous-time and discrete-time models with different structural assumptions. The general mathematically rigorous theory will be presented elsewhere (O.O. & I. H., manuscript in preparation).

The present structural model assumptions are justified as follows. The extinction rate is a function of the inverse of patch area, e/A_i, because large patches tend to have large expected population sizes and because extinction risk scales roughly as the inverse of the expected population size in taxa affected by moderate environmental stochasticity[9,28,29]. The colonization rate is given as a sum of contributions from the existing populations, $c\Sigma_{j\neq i}\exp(-\alpha d_{ij})A_j p_j(t)$, because immigration to patch i is expected to increase with the number of neighbouring populations, with their sizes as reflected by the respective patch areas, and with their decreasing distances to the focal patch and increasing incidences of occupancy.

Variation in patch quality and regional stochasticity

Instead of using patch area as a surrogate of expected population size, patch areas may be corrected, given sufficient information, for spatially varying habitat quality. Also, a simple but effective way of incorporating the consequences of regional stochasticity (spatially correlated environmental stochasticity) into the model is to replace the term $p_j(t)$ in the expression for colonization rate of patch i with a term such as $(1-\gamma\exp(-\beta d_{ij}))\,p_j(t)$. This term takes into account the fact that if extinctions are caused by regional stochasticity, the probabilities of patches i and j being empty become increasingly positively correlated. In addition, a negative correlation increasing λ_M may emerge if there exists an interaction between habitat quality and regional stochasticity (different patches are 'good' and 'bad' in different years).

Relative patch values

The contribution of patch i to λ_M can be closely approximated by $\lambda_i \equiv x_i^2\lambda_M$ (O.O. & I. H., manuscript in preparation) where x_i is the ith element in the leading eigenvector of matrix $\mathbf{M}$ (the values of x_i^2 are scaled to sum up to unity). The addition to λ_M that would be obtained by adding a new patch with area A_k to a specific location in the landscape can be calculated as

$$\lambda_k = \frac{A_k^2}{\lambda_M}\left(\sum_{j\neq k} e^{-\alpha d_{jk}} A_j x_j\right)^2 \qquad (6)$$

where d_{jk} is the distance from the existing patch j to the hypothetical patch k. Note that λ_k is defined as a product of contributions from patch area and spatial location, hence the advantage of having a new patch in a particular spatial location in the landscape can be evaluated independently of its area (Fig. 1: the network used in this example is one of the networks occupied by the Glanville fritillary butterfly in the Åland Islands in southwest Finland[30]).

The local value of patches labelled a–g in Figs. 1b and d was calculated for circular areas centred on the respective patch and with a radius of 0.5, 1.0, 1.5, … ($\alpha = 1$). For each circle, the values of λ_i and λ_M were calculated and displayed in Fig. 2. At the largest scale, when the circle around each patch includes all the other patches, the values converge to the global values shown in Fig. 1c. The intersection point of each patch-specific line joining the points (λ_i, λ_M) with the threshold condition (broken line in Fig. 2) gives the radius of the circle around patch i within which the threshold condition for metapopulation persistence is satisfied; in the case of patches a and c the threshold condition is satisfied with the smallest radius, 0.5. Figure 1b shows these areas for patches a–g. In Fig. 1d, which shows the result with regional stochasticity (see above in Methods), the radius of the circle corresponds to the same ratio δ/λ_M as in Fig. 1b.

Parameter estimation

For a metapopulation at stochastic steady state, the model can be parameterized using the formula $\delta = \lambda_M(1-p_\lambda^*)$. In the example in Fig. 3, the value of p_λ^* was calculated based on patch areas, spatial locations and the occurrence of the butterfly in the patches in 1993, the last providing (rough) empirical estimates of the p_i^* values. Only networks in the western Åland were included (network mid-point west of the longitude 310400 in the Finnish Uniform Coordinate System), as our previous analyses have indicated that many metapopulations in the eastern Åland were either severely out of the steady state or there are some environmental differences influencing patch occupancy[30]. For calculating λ_M, the value of $\alpha = 1$ was used, as estimated in mark–release–recapture studies[30].

Habitat loss

The results in Fig. 4 were calculated for hypothetical landscapes with 100 randomly located patches within an area of 5 by 5 units. The systematic loss of patches was obtained by reducing the area of the square from the margins and eliminating the patches that were located outside the reduced area. Patch areas are log-normally distributed. Model parameters have the values $\alpha = 1$ and $\delta = 0.3$. Results were calculated for 10 replicates, with the thick line showing the average. Patch areas in the replicates were scaled to give $\lambda_M = 1$.

Received 10 November 1999; accepted 14 February 2000.

1. Turner, M. G., O'Neill, R. V., Gardner, R. H. & Milne, B. T. Effects of changing spatial scale on the analysis of landscape pattern. *Landscape Ecol.* **3,** 153–162 (1989).
2. Turner, M. G. & Gardner, R. H. (eds) *Quantitative Methods in Landscape Ecology* (Springer, New York, 1991).
3. Gardner, R. H., O'Neill, R. V. & Turner, M. G. in *Humans as Components of Ecosystems: Subtle Human Effects and the Ecology of Population Areas* (eds Pickett, S. T. A. & McDonnell, M. J.) 208–226 (Springer, New York, 1993).
4. Lavorel, S., Gardner, R. H. & O'Neill, R. V. Analysis of patterns in hierarchically structured landscapes. *Oikos* **67,** 521–528 (1993).
5. Gustafsson, E. J. Quantifying landscape spatial pattern: what is the state of the art? *Ecosystems* **1,** 143–156 (1998).
6. Bascompte, J. & Solé, R. V. Spatially induced bifurcations in single-species population dynamics. *J. Anim. Ecol.* **63,** 256–264 (1994).
7. Gustafson, E. J. & Gardner, R. H. The effect of landscape heterogenity on the probability of patch colonization. *Ecology* **77,** 94–107 (1996).
8. With, K. A., Gardner, R. H. & Turner, M. G. Landscape connectivity and population distributions in heterogeneous landscapes. *Oikos* **78,** 151–169 (1997).
9. Hanski, I. *Metapopulation Ecology* (Oxford Univ. Press, Oxford, 1999).
10. Anderson, R. M. & May, R. M. *Infectious Diseases of Humans: Dynamics and Control* (Oxford Univ. Press, Oxford, 1991).
11. Levins, R. Some demographic and genetic consequences of environmental heterogeneity for biological control. *Bull. Entomol. Soc. Am.* **15,** 237–240 (1969).
12. Lande, R. Extinction thresholds in demographic models of territorial populations. *Am. Nat.* **130,** 624–635 (1987).
13. May, R. M. The role of ecological theory in planning reintroduction of endangered species. *Symp. Zool. Soc. London* **62,** 145–163 (1991).
14. Nee, S. & May, R. M. Dynamics of metapopulations: habitat destruction and competitive coexistence. *J. Anim. Ecol.* **61,** 37–40 (1992).
15. Lawton, J. H., Nee, S., Letcher, A. J. & Harvey, P. in *Large-scale Ecology and Conservation Biology* (eds Edwards, P. J., May, R. M. & Webb, N. R.) 41–58 (Blackwell Scientific, Oxford, 1994).
16. Hill, M. F. & Caswell, H. Habitat fragmentation and extinction thresholds on fractal landscapes. *Ecol. Lett.* **2,** 121–127 (1999).
17. With, K. A. & King, A. W. Extinction thresholds for species in fractal landscapes. *Conserv. Biol.* **13,** 314–326 (1999).
18. Hanski, I. & Gyllenberg, M. Uniting two general patterns in the distribution of species. *Science* **275,** 397–400 (1997).
19. Hanski, I. A practical model of metapopulation dynamics. *J. Anim. Ecol.* **63,** 151–162 (1994).
20. Grenfell, B. T. & Dobson, A. P. (eds) *Ecology of Infectious Diseases in Natural Populations* (Cambridge Univ. Press, Cambridge, 1995).
21. Adler, F. R. & Nüernberger, B. Persistence in patchy irregular landscapes. *Theor. Pop. Biol.* **45,** 41–75 (1994).
22. Lindenmayer, D. B. & Possingham, H. P. *The Risk Of Extinction: Ranking Management Options For Leadbeater's Possum Using Population Viability Analysis* (Centre for Resource and Environmental Studies, Canberra, 1994).
23. Hanski, I. in *The Ecological Basis of Conservation* (eds Pickett, S. T. A., Ostfeld, R. S., Shachak, M. & Likens, G. E.) 217–227 (Chapman & Hall, New York, 1997).
24. Freitag, S. & van Jaarsveld, A. S. Sensitivity of selection procedures for priority conservation areas to survey extent, survey intensity and taxonomic knowledge. *Proc. R. Soc. Lond. B* **265,** 1475–1482 (1998).
25. Pressey, R. L., Possingham, H. P. & Margules, C. R. Optimality in reserve selection algorithms: when does it matter and how much? *Biol. Conserv.* **76,** 259–267 (1996).
26. Nee, S. How populations persist. *Nature* **367,** 123–124 (1994).
27. Hanski, I. Metapopulation dynamics. *Nature* **396,** 41–49 (1998).
28. Lande, R. Risks of population extinction from demographic and environmental stochasticity and random catastrophes. *Am. Nat.* **142,** 911–927 (1993).
29. Foley, P. Predicting extinction times from environmental stochasticity and carrying capacity. *Conserv. Biol.* **8,** 124–137 (1994).
30. Hanski, I., Moilanen, A., Pakkala, T. & Kuussaari, M. The quantitative incidence function model and persistence of an endangered butterfly metapopulation. *Conserv. Biol.* **10,** 578–590 (1996).

Acknowledgements

We thank N. Behera, K. Frank, B. Grenfell, M. Keeling, A. Moilanen, B. O'Hara, T. Roslin, I. Saccheri and C. Thomas for comments on the manuscript.

Correspondence and requests for materials should be addressed to I. H. (e-mail: ilkka.hanski@helsinki.fi).